

QUANTUM WELL AND QUANTUM BARRIER DIODES FOR GENERATING SUB-MILLIMETER WAVE POWER.

Hans Grönqvist*, Erik Kollberg* and Anders Rydberg**.

The Millimeter Wave Laboratory

Departments of Applied Electron Physics* & Radio and Space Science**

Chalmers University of Technology

S-412 96 Göteborg, Sweden

Abstract.

Quantum well diodes have been used for generating power at millimeter and submillimeter waves, both in negative resistance oscillators and in multipliers. In this paper, we will first discuss the power versus frequency and the maximum frequency of oscillation of "ordinary" quantum well oscillators. Possible methods of improving the power output and the maximum frequency of oscillation will be suggested. Quantum well diode multipliers will also be discussed. Realizing the importance of the non-linear capacitance for the quantum well diode multiplier efficiency we have investigated a quantum barrier diode in multiplier applications.

1. Introduction.

Quantum Well diode (QW-diode) oscillators have recently been shown to have a potential to generate power in the millimeter and submillimeter wave region [1,2]. The device used in these oscillators is a kind of tunnel diode with negative differential resistance, first suggested as early as 1970 by Esaki. They were, however, not implemented experimentally until 1974, [3], when MBE (Molecular Beam submillimeter) technique for making appropriately doped epitaxial Ga(Al)As was developed. The first experiments with QW diode oscillators were made by Sollner 1983 at microwave frequencies. The best QW oscillator results so far have been reported by Sollner et. al. [1] and by us [2]. The QW-diode can also be used in multipliers [4], and should have a possible application in negative resistance mixers with a potential of having conversion gain [5].

In paragraph 11 we will describe a new device, the *Quantum Barrier Varactor* (QBV) diode multiplier, which has high efficiency and interesting properties since only odd harmonics are created.

2. Device design.

A typical outline of a QW-diode is shown in Fig. 1. The doping profile and the band bending for a biased diode is shown in Fig. 2a. The tunneling current has a maximum for the bias voltage making the energy level in the well equal in energy with the Fermi level to the left of the QW. An approximate equivalent circuit of the QW-diode is shown in Fig. 2b. The parameters in the equivalent circuit are depending on the doping profile, bias conditions, and size of the diode. There are several possibilities to increase the output power. It has been suggested that more power will be available if the $\Delta I \cdot \Delta V$ product (ΔI and ΔV are the differences in current and voltage respectively, measured

between the peak and valley current points of the iv-characteristic) approximately determined from the iv-characteristic) can be increased by improving the device. However, the analysis given below, shows that ΔI is more fundamental than ΔV .

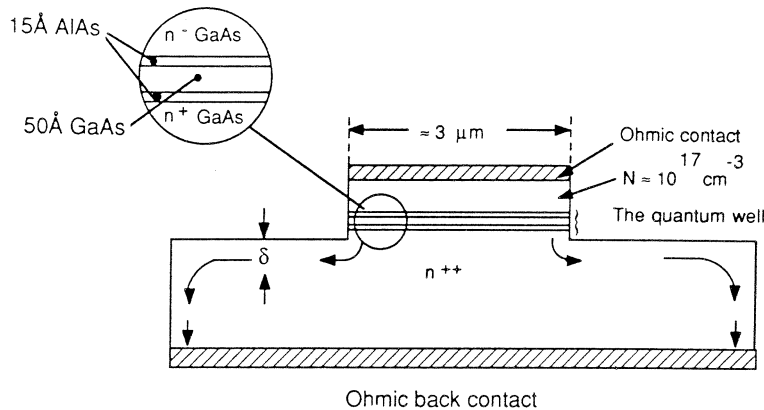


Fig. 1. Schematic diagram of a typical QW-diode.

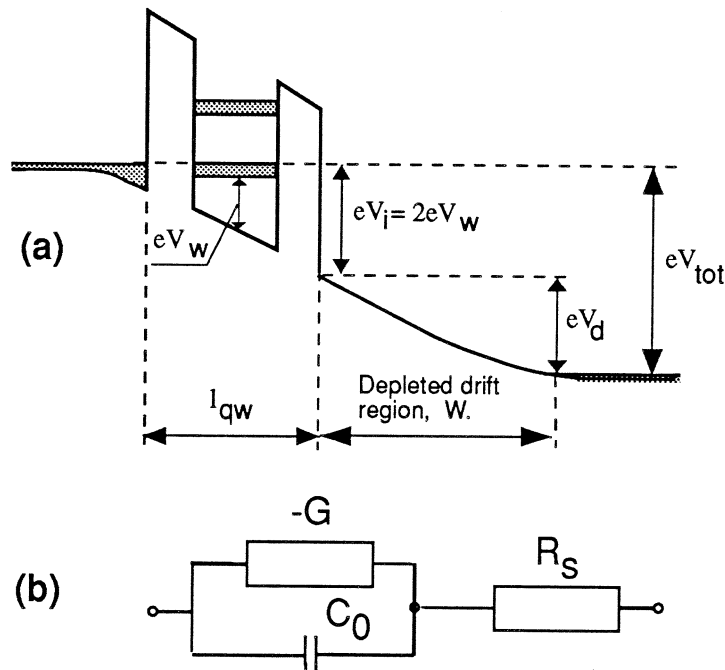


Fig. 2. Electron potential energy at the conduction band edge for a forward bias of $V_{tot} = V_{qw} + V_d$ (a), and the equivalent circuit (b).

3. The maximum frequency of oscillation.

A simplified equivalent circuit of a QW diode oscillator is shown in Fig. 3. When the oscillator starts oscillating, the voltage amplitude ΔV_{OSC} will increase and the effective negative conductance G_{eff} will decrease until the requirements of the oscillator are satisfied, i. e. ΔV_{OSC} will adjust itself so that [6]

$$G_{eff} = \frac{1}{2(R_l + R_s)} \cdot (1 - \sqrt{1 - [2(R_l + R_s)\omega C_o]^2}) \tag{1}$$

which requires $2(R_l + R_s)\omega C_o < 1$ i.e.

$$f < \frac{1}{4\pi(R_l + R_s)C_o} < \frac{1}{4\pi R_s C_o} \tag{2}$$

Hence, the maximum frequency of oscillation is

$$f_{max} = \frac{1}{2\pi} \cdot \frac{1}{2R_s C_o} \tag{3}$$

For this frequency the load resistance is zero, i.e. no power is delivered to the load. For low frequencies $G_{eff} \approx (R_l + R_s)(\omega C_o)^2$, and hence

$$G_{eff\ min} \approx R_s (\omega C_o)^2 \tag{4}$$

which ensures the largest possible voltage swing and maximum power at ω . G_{eff} will evidently increase with increasing frequency while the voltage swing will decrease. This phenomenon is illustrated in Fig. 4.

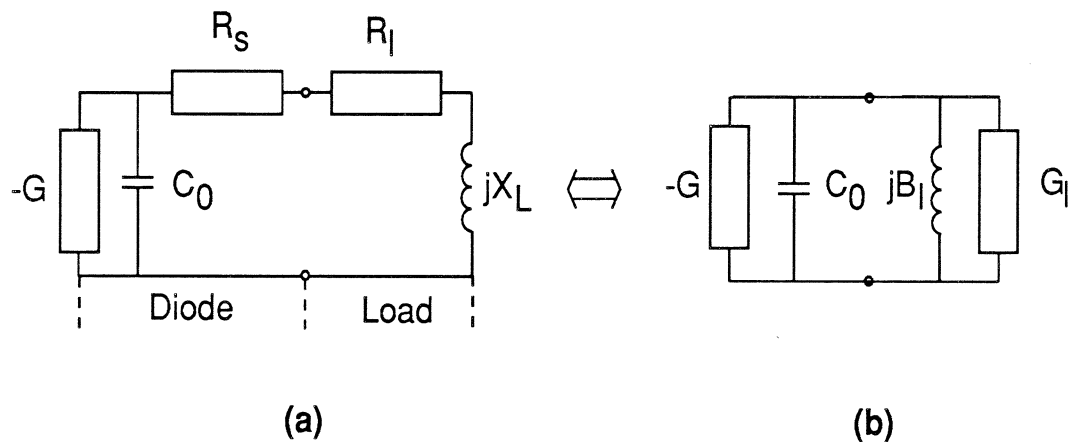


Fig. 3. Equivalent circuit of a QW-diode oscillator (a), and the derived equivalent parallel circuit (b) (to be used for evaluating relevant oscillator properties).

Both the diode negative conductance and the parallel capacitive susceptance are affected by the drift region and the space charge related to the conduction current through the diode. Assuming that the frequency is low in the sense that the drift angle $\theta = \omega W/v_s$ (where W is the length of the drift region, v_s is the mean velocity of the electrons traveling through the drift region) is small ($\leq \pi/3$) we may assume that the *large signal* admittance of the drift region can be expressed in the same way as for the

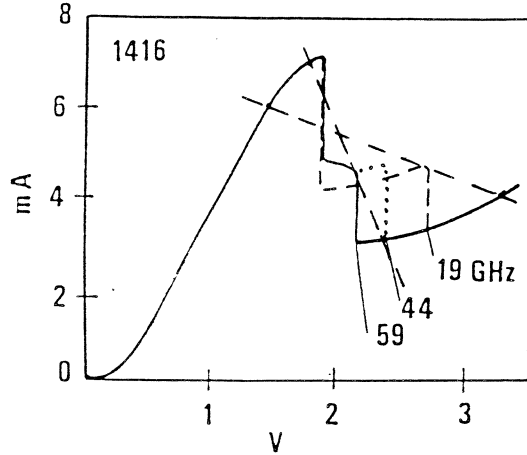


Fig. 4. DC iv-characteristic of a QW-diode in a 19, 44, and 59 GHz oscillator (from ref. [2]). The load-lines defined as $(1/G_1 - R_s)$ (see paragraph 4 below) for 19 and 59 GHz are also shown.

small signal case, i.e. [6]:

$$Y = G + jB \quad (5)$$

$$G \approx A \cdot \left(\frac{W}{\sigma_e} + \frac{W^2}{2 \epsilon v_s} \right)^{-1} = \frac{A \cdot \sigma_e}{W} \left[1 + \frac{\sigma_e W}{2 \epsilon v_s} \right]^{-1} \quad (6)$$

$$jB \approx A \cdot \left(\frac{W}{j \omega \epsilon} + \frac{\sigma_e W^2}{j \omega \epsilon 2 \epsilon v_s} \right)^{-1} = j \frac{A \omega \epsilon}{W} \left[1 + \frac{\sigma_e W}{2 \epsilon v_s} \right]^{-1} \quad (7)$$

where σ_e is then an effective (*large signal*) negative conductance related to the well region and characteristic of the oscillating diode and A the area of the diode. In these expressions the influence from the delay of the rf current with respect to the rf voltage is neglected. The term $\sigma_e W / 2 \epsilon v_s$ in equation (6) and (7) is due to the space charge. The effective capacitance of the diode is consequently larger for $\sigma_e < 0$ than the "cold" capacitance $A \epsilon / W$. If the space charge term is large enough, it may cause a hysteretic form of the iv-characteristic [6]. Eq. (6) and (7) can also be derived using the impedance expression given in ref. [7], and using the same approach as in [6], we have found them approximately valid also for a punch through diode, i.e. the "depleted" drift region will reach the n^{++} -region.

When the diode oscillates, the oscillating voltage amplitude and current amplitudes adjust, i.e. σ_e obtains a certain value, such that $|G| = G_{\text{eff}}$ (see Eq.(1)). Hence, σ_e is determined. At the maximum frequency of oscillation, $R_1 = 0$ and $|G| = 1/2 R_s$, yielding a particular value for σ_e , which can be put into Eq.(7) for determining jB . Realizing that $j \omega C_0 \equiv jB$, we now obtain for the maximum frequency of oscillation

$$f_{\text{max}} \approx \frac{1}{4 \pi R_s C_0} = \frac{W}{4 \pi R_s A \epsilon} \left(1 + \frac{W^2}{4 A \epsilon v_s R_s} \right)^{-1} \quad (8)$$

Notice that R_s and A are inter-related and that v_s is a complicated function of W [12]. If R_s is dominated by the mesa contact resistance, $R_s \cdot A$ is approximately constant, and f_{max} is therefore independent of the diode area. However, in practice there are further contributions to R_s such as the spreading

resistance [8]. If A and R_s are fixed, and knowing $v_s(W)$, W can be optimized (either by choosing a certain doping concentration N_D which will determine the width of the depleted region, W , or designing the diode so that the drift region is "punch through" to the highly doped region). The capacitive susceptance jB for frequencies below f_{\max} corresponds to a susceptance of $B=(1/2R_s)(f/f_{\max})$.

Eq.(8) does not take into account the negative conductance $-G_{qw}$ and the susceptance B_{qw} of the QW itself. This influence is easily included, since the ratio $-G_{qw}/B_{qw} = -G/B$ [Eqs.(6) and (7)]. The conclusion is that Eq.(8) can just be modified so $W \rightarrow W+l_{qw}$ and $v_s \rightarrow v_s (1+l_{qw}/W)^2$ where l_{qw} is the extension of the QW (see Fig. 2). Consequently f_{\max} will increase typically 10% by taking into account the influence of $-G_{qw}$ and B_{qw} . Evidently R_s and v_s are very important parameters for reaching the highest possible frequencies. In fact, the maximum frequency of oscillation will have a maximum, which for $R_s = 10 \Omega$ and $v_s=0.6 \cdot 10^5$ m/s is 290 GHz with $W = 700 \text{ \AA}$, and for $R_s = 20 \Omega$ is 210 GHz with $W = 830 \text{ \AA}$. Similar results as obtained with equation (8) were obtained by Brown et. al. [9]. We will return to this discussion in paragraph 8 below. Notice also that f_{\max} is finite for $R_s = 0$. In this case, the power is dissipated in the space-charge resistance, $R_{spch}=W^2/(2 \cdot A \epsilon v_s)$ (see e.g. Ref.[6] or [7]). In fact, f_{\max} can be expressed as (changing $W \rightarrow W+l_{qw}$ and $v_s \rightarrow v_s(1+l_{qw}/W)^2$):

$$f_{\max} \approx \frac{W + l_{qw}}{4\pi A \epsilon (R_s + R_{spch}/2)} \quad (9)$$

with

$$R_{spch} = \frac{(W+l_{qw})^2}{2 A \epsilon v_s} \quad (10)$$

4. Output power of the fundamental oscillator.

Let us assume that the oscillating current and voltage amplitudes adjust themselves such that Eq. (1) is satisfied, and that the rf current amplitude i_{rf} passing through the the negative conductance of the diode is the same as observed at DC, i.e. $i_{rf} = \Delta I/2$. At resonance this current must also pass through the load conductance G_l (Fig. 3b). The maximum power delivered to the load can then be calculated. Since $G_l (= G_{\text{eff}} \text{ of eq. (1)})$ is a function of R_l we obtain using eq. (1)

$$P_{\text{del}} = \frac{\Delta I^2}{8} \frac{1}{G_l} \cdot \frac{R_l}{R_l + R_s} = \frac{\Delta I^2}{4} \frac{R_l}{1 - \sqrt{1 - [2(R_l + R_s)\omega C_0]^2}} \quad (11)$$

which increases with R_l and becomes maximum when

$$1 - 2(R_l + R_s) \omega C_0 = 0 \quad (12)$$

The load conductance G_l approximately equals G of Eq.(6) and the ωC_0 approximately equals B of Eq.(7). In a similar way as Eq.(9) is derived, one obtains now for the oscillation frequency

$$f = \frac{W + l_{qw}}{4\pi A \epsilon (R_l + R_s + R_{spch}/2)} \quad (13)$$

and from Eq.(13), (3) and (9) one obtains

$$R_{\text{lopt}} = R_{\text{spch}} \frac{v_s}{W+l_{\text{qw}}} \left(\frac{1}{f} - \frac{1}{f_{\text{max}}} \right) \quad (14)$$

with which Eq.(11) and (12) yields the maximum power into R_1 as

$$P_{\text{delmax}} = \frac{\Delta I^2}{8} \frac{W}{A\epsilon} \left(\frac{1}{f} - \frac{1}{f_{\text{max}}} \right) \quad (15)$$

This equation is different to Eq.(20) of Ref.(6), the reason being that in Ref.(6) C_0 was assumed constant and equal to the value for $f = f_{\text{max}}$. Noticing that ΔI is proportional to A , P_{delmax} as expected is proportional to the diode area A .

Eqns.(11)-(15) must be handled with some care. Eq.(15) seems to suggest that the power output goes to infinity for $f = 0$. The reason is that the model assumes the voltage swing ΔV over the diode to be $\Delta I/G_1 = \Delta I/G_{\text{eff}}$, which is quite unrealistic when ΔV becomes significant larger than the voltage difference between at the peak and the valley current. It is obvious that zero load resistance leads to zero output power and too large load resistance means no oscillations.

5. Comparison with experiments.

Referring to our own work [10], mesa diodes with a diameter of $\approx 4 \mu\text{m}$ and a height of $\approx 0.5 \mu\text{m}$ were fabricated. Two different epitaxial designs have been tested so far. Diode #1 consists of 45 Å GaAs well surrounded by 20 Å AlAs barriers and a 50 Å spacer layer of GaAs outside each barrier. All of these layers are nominally undoped. Outside the spacer layers a region of low doped GaAs, Si doped to $2 \cdot 10^{17} \text{ cm}^{-3}$, with a length of 2000 Å is grown. The second diode, #2, differs in mainly one aspect: the region of low doping ($6 \cdot 10^{16} \text{ cm}^{-3}$) is 2250 Å, and grown on one side only.

The diodes were tested in both post and cap waveguide mount structures. We found that output power of the QW-diode #1 often was a harmonic, with the fundamental oscillation frequency below the cut-off frequency of the waveguide. Such harmonic operation modes were found to be due to resonances caused by the bias circuit of the mount. By improving the bias circuit it was possible to obtain fundamental oscillations at frequencies within the waveguide transmission band. In Fig. 5 is the output power as obtained from Eq. (15) compared with the experimental results for fundamental oscillations reported in ref. [2]. In these experiments we carefully checked if any subharmonic power could be detected in the bias circuit, as was the case for the "harmonic mode operation". Notice that the theoretical power is obtained choosing the load resistance R_{lopt} for maximum output power i.e. using Eq.(14)-(15). The experimental output powers are (of course) lower. By optimizing the embedding impedance of the mount, reducing the series resistance of the device and the losses in the mount, more output power should be achieved. Moreover, judging from our experiments and assuming that it should be realistically possible to match the circuit to a diode with $\text{Re}\{Z_0\} = 1 \Omega$, it should be possible to increase the diode area with a factor of 70. Hence, the output power also should improve with a factor of approximately 70 (compare Fig. 5) to about 6 mW at 100 GHz.

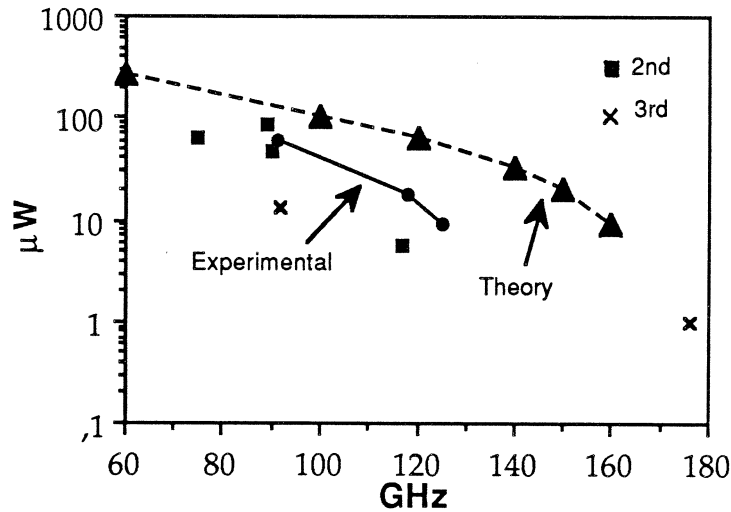


Fig. 5. The output power for a fundamentally oscillating optimized quantum well oscillator according to eq. (11) and as obtained experimentally (from ref. [2]). It is assumed that $A = 1.2 \cdot 10^{-11} \text{ m}^2$, $R_S = 20 \Omega$, $W = 1100 \text{ \AA}$, and $\Delta I = 4 \text{ mA}$. Also shown is the experimentally obtained output power for oscillators at the 2nd and the 3rd harmonic (also from ref. [2]).

An educational case is illustrated by the properties of the diode #2 with the low doping and a long depleted drift region. Quite a large space charge resistance is obtained for this diode. The i - v -characteristic shows a large hysteresis, and the highest frequency of oscillation obtained experimentally (it was very difficult to get oscillations) was as low as 100 MHz. It was found that the measured hysteresis fits very well to what can be expected from the available fabrication data of the diode assuming it to be due to space charge effects. Applying Eq.(10) assuming $v_s = 6 \cdot 10^4 \text{ m/s}$ and $R_S = 20 \Omega$ yields $f_{\text{max}} = 95 \text{ GHz}$.

The i - v -characteristic shown in Fig. 4 is typical and obtained with diode #1. It shows hysteresis as well as a characteristic step at the negative resistance slope part. Both phenomena can be explained assuming oscillations. The step can be explained as a mean current for this bias voltage range when the diode is experiencing oscillations. If the voltage swings approximately between the maximum peak current and the valley minimum, the resulting current should be of the order the mean of the maximum and the minimum current, as observed. The hysteresis is caused by the fact that oscillations can start as soon as the small signal negative σ ($= di/dv$ in the bias point) has a large enough amplitude, and that oscillations once started may continue even if the small signal σ at the bias point is positive. This is due to the fact that for large voltage swing at increased bias the *effective* σ_e remains negative [6].

It is interesting too, to determine the load line, G_{eff}^{-1} for the oscillating diodes of Figure 4. The load line of the *active* part of the diode (the series resistance not included as part of the diode) is $(R_{\text{lopt}} + R_S)$, yielding 800Ω for 19 GHz, 290Ω for 44 GHz and 180Ω for 59 GHz. In Figure 4 these load-lines are indicated (it would have been more accurate to modify the dc- i - v -characteristic by subtracting the voltage drop over the series resistance, $i_{\text{dc}} \cdot R_S$).

6. Harmonic output power.

As already mentioned the nonlinear i - v -characteristic and a large oscillation voltage amplitude will cause a large harmonic content in the resulting current waveform. Hence at "low" fundamental oscillation frequencies, when the voltage amplitude surely is large, the oscillator ought to be very efficient as a harmonic oscillator. Due to the symmetry of the i - v -characteristic, the 3rd harmonic should have a comparatively large amplitude. This also agrees with the result shown in Fig. 5. Besides the nonlinearity of the i - v -characteristic itself, another reason for a large harmonic content, is relaxation type oscillations (see e.g. Ref. [11]). One cannot expect a pure sinusoidal oscillation at any frequency, not even at the highest possible frequency of oscillation. Hence, one concludes that when output power is required at frequencies near and above f_{\max} it is more advantageous to design the oscillator as a harmonic oscillator. The optimum fundamental oscillating frequency is then probably to be chosen at $f_{\text{osc}} \approx (1/3) \cdot f_{\text{out}}$.

Also notice that the current amplitudes at the harmonic frequencies should remain large up to frequencies *well above the maximum frequency of oscillation*. Important for the performance are the actual embedding impedances at these frequencies and the capacitance of the diode. Efficient multiplication should therefore be possible to obtain to quite high output frequencies.

7. Optimizing the diode.

The drift length over which the carriers have high velocity is limited and is a function of the electric field after the barrier and the injection energy. In Fig. 6 is shown f_{\max} vs the length of the drift region for different mean velocities. Notice that the Figure may be used for other values of the series resistance than 10Ω . For e.g. $R_s = 5 \Omega$ (20Ω), multiply (divide) the velocities and the frequency scale with 2.

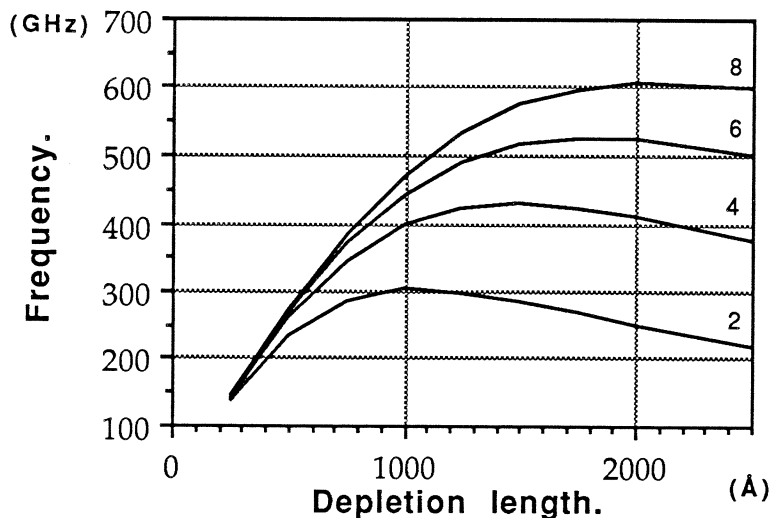


Fig.6. Calculated values for f_{\max} as a function of depletion length for different carrier velocities using Eq.(11). The values for v ranges from $2 \cdot 10^5$ m/s to $8 \cdot 10^5$ m/s. The area A of the diode is $12 \mu\text{m}^2$ and the series resistance R_s is 10Ω .

For "ordinary" GaAs diodes a frequency of ≈ 600 GHz could probably be reached with a depletion length of 600 \AA ($W+l_{\text{qw}}=700 \text{ \AA}$). However, in order to achieve this or higher frequencies, one must understand the fundamental problems in this context. We will also show that if InAs is used in the drift region, the higher achievable velocities will ensure a still higher f_{max} .

8. Optimizing the GaAs diode design.

In GaAs, electrons subjected to an electric field will travel much faster in the main Γ valley than in the L valley. Since the energy of the L valley is 0.31 eV above the bottom of the Γ valley it can be concluded that when carriers in an accelerating field have gained energy $\geq 0.31 \text{ eV}$, a transfer of the carrier to a higher valley will occur, and the velocity of the carrier drops. Monte Carlo simulations for GaAs [12] do show a velocity decrease when this requirement is fulfilled. Hence as a rule of thumb, the requirement

$$e \cdot V_{\text{peak}} \approx 0.31 \text{ eV} \quad (16)$$

should be fulfilled in order to maintain a high mean velocity through the drift region. The peak current voltage is the sum of the voltage over the accumulation layer in front of the QW, the voltage drop V_{qw} over the QW itself and the voltage drop V_{d} over the drift region. From Fig. 2 and simple geometrical arguments it is obvious that the injection energy for *peak current* and a symmetric double barrier structure $e \cdot V_{\text{i}}$ is related to the electron excess energy eV_{w} in the well viz. $eV_{\text{i}} = 2 \cdot e \cdot V_{\text{w}}$ ($=e \cdot V_{\text{qw}}$) and the accelerating field E_{w} in the drift region at the quantum well is

$$E_{\text{w}} = \frac{2 \cdot V_{\text{w}}}{(L_{\text{w}} + 2L_{\text{b}})} \quad (17)$$

where L_{w} and L_{b} are the width of the well, and the width of the barriers respectively. If the potential in the drift region is parabolic, the voltage drop over the drift region becomes $V_{\text{d}} \approx 0.5 \cdot L_{\text{d}} \cdot E_{\text{w}}$ where L_{d} is the length of the drift region. Hence with equation (17) the requirement for the mean velocity to be as high as possible is

$$2V_{\text{w}} \cdot \left(\frac{L_{\text{d}}}{2(L_{\text{w}} + 2L_{\text{b}})} + 1 \right) \approx 0.31 \text{ eV} \quad (18)$$

We propose two possible ways of decreasing V_{w} : **i.** lowering V_{w} by increasing the width of the well, and **ii.** lowering V_{w} by doping the well with indium.

In order to determine the effect of increasing the width of the well, we have solved the Schrödinger equation for different well widths and no bias (Fig. 7). The barriers are taken as AlAs, giving the potential barriers equal to 1 eV . The bold line indicate the present device with 45 \AA well width and the circles show the two energy levels in that well. Although when the device is biased the well region does no longer have a simple square shape, Fig. 7 yields a reasonable estimate of the real situation. As is seen in the figure, the energy levels are lowered as the width of the well is increased.

Another approach to lower the energy level is to grow the well region with a lower band gap than GaAs. For $\text{In}_x\text{Ga}_{1-x}\text{As}$ with small values of x , the difference in band gap is given by [13]

$$\Delta E = 0.2295x^2 - 1.1365x \tag{19}$$

in eV. Roughly 85% of this difference is in the conduction band, the rest in the valence band. The mixing of InAs with GaAs is slightly more complicated than the mixing of AlAs with GaAs since the lattice constant of InAs is different from that of GaAs. Thus a strained layer is formed and there is a limiting thickness to the layer that can be grown. This is discussed in [14] and it can be concluded that for a 45 Å well the maximum In content is ≈40%. The In-doping means that the potential barrier becomes higher, which should be accounted for in a more exact theoretical evaluation.

The best solution is to combine these methods and use a slightly wider well and a limited In content in the well.

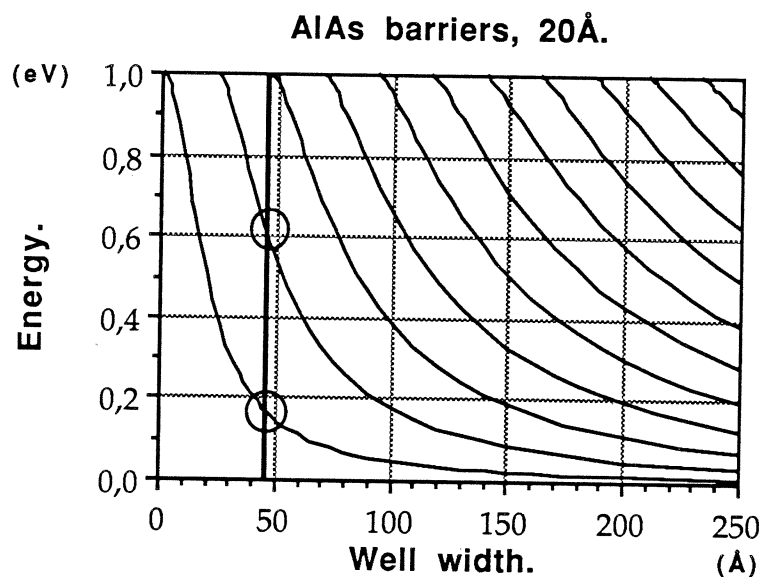


Fig.7. The energy levels for a square well potential for well widths up to 250Å. The bold line indicates the 45Å well currently used in the devices with the two energy levels, one at ≈0.17eV and one at ≈0.63eV.

In the table below, is given some examples on expected f_{max} of different designs all with diode areas of 12 μm². The original experimental diode yields an f_{max} of approximately 170 GHz.

Width Å	In %	V _w meV	E _w kV/cm	W _{opt} Å	v _s 10 ⁵ m/s	R _s Ω	f _{max} GHz	Rem.
45	0	170	400	1000	1.0	20	170	Exp.diode
45	0	170	400	1000	1.0	5	≈230	
60	0	110	220	600	1.0	5	≈300	
60	7	32	64	600	8.0	5	≈600	
60	8	22	44	800	3.0	5	≈500	
60	8	22	44	800	3.0	20	≈200	

The diode we have have used in experiments was according to the upper one in the table, i.e. f_{max} was as low as 170 GHz. Improving the mean velocity by using In in the well and broadening the well itself, for the same series resistance f_{max} will become about 200 GHz, while if R_s can be 5 Ω, one may reach $f_{max} = 600$ GHz.

It is interesting to use Eq. (15) to predict the maximum output power at e. g. 400 GHz for the diode with $f_{\max}=600$ GHz of the table above ($W+l_{qw}=700$ Å, $v_s=6\cdot 10^5$ m/s) by choosing a larger area diode (R_s proportional to $1/A$). It is reasonable to assume at that 400 GHz it is realistically possible to match the diode to a $5\ \Omega$ load resistance. This should allow us to use a $60\ \mu\text{m}^2$ area diode ($R_s=1\ \Omega$, $\Delta I\approx 20$ mA) yielding a maximum output power (Eq. (15)) of approximately $420\ \mu\text{W}$. Probably only of the order $200\ \mu\text{W}$ will be available as useful output power. Whether it is possible to achieve still more output power at 400 GHz for a diode oscillating fundamentally at 133.3 GHz, is not clear. The maximum output power at 133 GHz for the same diode area should be about 7 times higher, i. e. 3 mW.

9. Using InAs in the drift region.

A way to get around the problem of decreasing velocity for electrons with high energies is to use a material combination where the lowest upper valley is higher up than the 0.31 eV in GaAs. The upper valley in InAs is more than 1 eV higher than the Γ valley [13] but this is not the sole benefit of that material system. The mobility is higher, $\approx 33000\ \text{cm}^2/\text{Vs}$ compared to $8500\ \text{cm}^2/\text{Vs}$ for GaAs at room temperature [15]. Moreover, the the series resistance in this material can be made lower, partly because the higher mobility but also since the band gap is lower it gives a lower ohmic contact resistance.

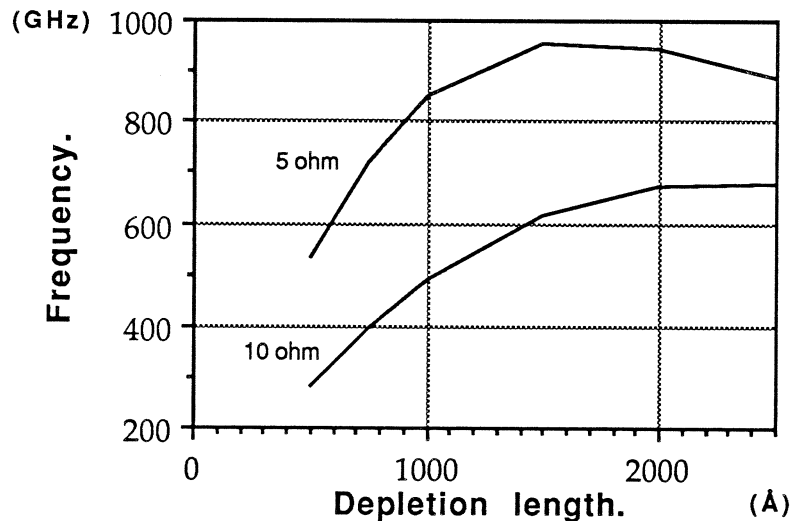


Fig. 8. Calculated values for f_{\max} as a function of depletion length for two different series resistances $5\ \Omega$ and $10\ \Omega$, assuming v_s is 10^6 m/s and the area A of the diode is $12\ \mu\text{m}^2$. These parameters are probably obtainable for InAs.

Experiments on this material system with quantum well diodes have been performed with good results [16]. Large peak to valley ratios can be obtained, since barriers of AlSb in InAs are very high, ≈ 1.3 eV, compared to ≈ 1 eV for AlAs barriers in GaAs. Even though this is a new material and hardly tested it looks to be the most promising for the future because of the possibility to get high carrier velocity and low series resistance. The peak velocity for bulk InAs is $\approx 3.6\cdot 10^5$ m/s [13], around 60%

higher than GaAs $\approx 2.2 \cdot 10^5$ m/s. For short distances in GaAs this peak velocity can be exceeded by two to three times, [12]. If the same is true for InAs the maximum velocity would be approximately $10 \cdot 10^5$ m/s, and this without the necessity of having a low field outside the barriers. Due to the lower bandgap of InAs as compared to GaAs, better ohmic contacts should be obtainable. In Fig. 8, calculated values for f_{\max} is presented with $v_s = 10 \cdot 10^5$ m/s and the series resistance $R_s = 10 \ \Omega$ and $R_s = 5 \ \Omega$. A maximum frequency is then ≈ 900 GHz for a $5 \ \Omega$

Finally it is interesting to use Eq. (15) to predict the the maximum output power at e. g. 750 GHz for an optimized InAs diode with $f_{\max} = 900$ GHz (assuming $W + l_{\text{qw}} = 1500 \ \text{\AA}$, $v_s = 10 \cdot 10^5$ m/s, $R_s \approx 6 \ \Omega$ for a $12 \ \mu\text{m}^2$ area). Assuming that at this frequency it is possible to match the diode to a load resistance of $10 \ \Omega$ (higher losses causes a larger load resistance), the maximum power to the load (Eq. (15)) will be of the order $250 \ \mu\text{W}$. Probably only a fraction of this power (may be 50 %) will be useful. The optimum area of this diode is then about $15 \ \mu\text{m}^2$, $R_s \approx 4.6 \ \Omega$ and $\Delta I \approx 10$ mA. If a still lower R_s is possible to realize, of course still higher output powers can be achieved.

10. QW-diode Multipliers.

As was pointed out in paragraph 6, the QW oscillator may be very rich in harmonics. One should therefore expect potential high efficiency from a QW diode multiplier. We have designed a Quantum Well (QW) diode frequency tripler with more than 1.2 % efficiency and 0.8 mW output power at about 250 GHz [4]. A comparison between the experimental results and the theoretically calculated efficiency for a tripler using such a diode has been made. The multiplier mount used in our experiments is meant for Schottky-varactor triplers, and has a design similar to Erickson's [17]. Due to the symmetric I-V characteristic of the QW-diode, see Figure 9, only odd harmonics are obtained for zero bias voltage using the QW in a multiplier. This means that the current of a QW-diode pumped by a sinusoidal signal contains mainly third and fifth harmonics. Thus the idler tuning used in this mount at the second harmonic is of no importance in this case if the bias voltage is zero. In Figure 10 the measured efficiency versus input power for the QW-diode at three different output frequencies is plotted. It can be seen that the efficiency increases with input power up to a certain level where it becomes more or less saturated. Maximum efficiency was obtained for zero voltage bias.

Using the large signal multiplier analysis program developed by Siegel et al. [18] and modified by us for the QW-diode, the efficiency of the diode was calculated as a function of the input power. A simple equivalent circuit consisting of a non linear capacitance in parallel with a nonlinear resistance was assumed for the QW-diode. A series resistance represents frequency dependent (due to the "skin effect") losses. The capacitance of the diode was assumed to vary inversely as a function of the length L of the depletion region. The parallel resistance of the QW-diode was assumed to follow the measured I-V characteristic of the diode, see Figure 9. The frequency dependent series resistance of the QW-diode was calculated to be between 22 - $32 \ \Omega$ (at 83 GHz) depending on the contact resistance (measured to be between $2 \cdot 10^{-6}$ - $4 \cdot 10^{-6} \ \Omega\text{cm}^2$) of the chip.

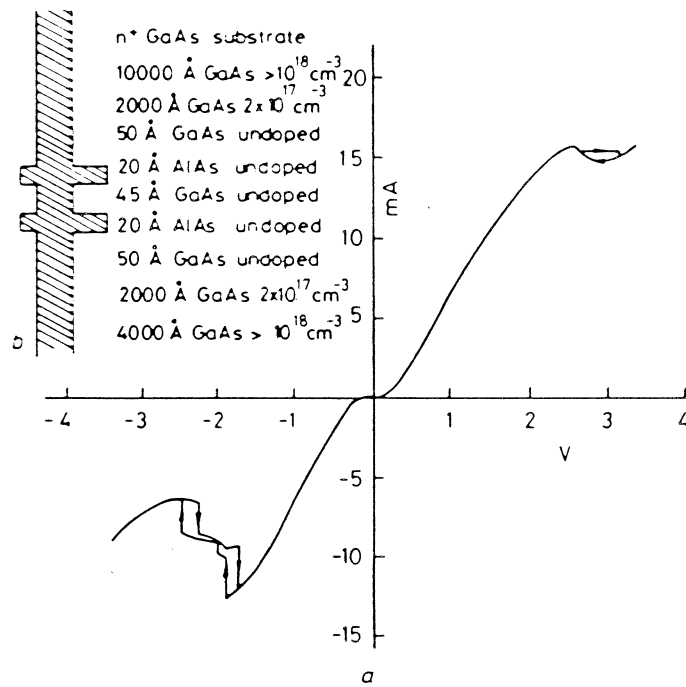


Fig. 9. The IV-characteristic of the QW-diode used in the multiplier experiments.

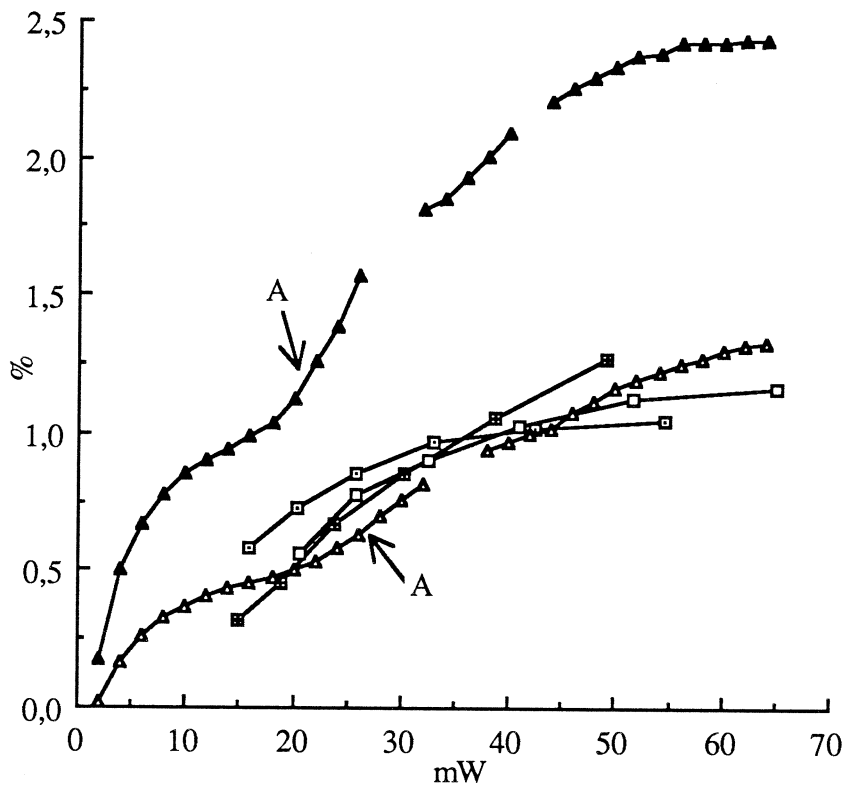


Fig. 10. Measured and calculated efficiency vs input power for the tripler.
 (□): measured efficiency at 242 GHz.
 (■): measured efficiency at 249 GHz.
 (▴): measured efficiency at 257 GHz.
 (▲): calculated efficiency for 249 GHz, contact resistance is $2 \cdot 10^{-6} \Omega \text{cm}^2$.
 (△): calculated efficiency for 249 GHz, contact resistance is $4 \cdot 10^{-6} \Omega \text{cm}^2$.

The theoretically calculated results at an output frequency of 249 GHz are shown in Figure 10 for -0.2V bias voltage (\approx zero bias). It is seen that one for a contact resistance of $4 \cdot 10^{-6} \Omega \text{cm}^2$ the experimental and theoretical curves agree. However, due to the negative differential resistance above about 2V (see Figure 9) the program did not always converge, as indicated by the broken line curve in Figure 10.

At the points "A" in Figure 10 the theoretically calculated efficiency starts to increase. This is due to the voltage swing of the pump signal across the QW-diode exceeds the voltage for peak current in the I-V characteristic of the diode, see Figure 9. Thus the negative differential resistance portion of the I-V characteristic of the QW enhances the efficiency of the tripler.

It can be seen that the general behaviour of the theoretical curves agree well with the measured ones. Thus the simple equivalent circuit applied here for the QW-diode could be used as a first approximation for the diode. The equivalent circuit of the QW-multiplier is further investigated in Ref. [19].

11. QBV-diode multipliers.

A new device, the Quantum-Barrier-Varactor diode (QBV-diode), has been proposed by us for use in multipliers for millimeter-waves [20]. Since the capacitance vs voltage characteristic is symmetric, only odd harmonics are obtained. Hence there is no idler circuit to consider for the tripler and only one for the quintupler. It is shown that for triplers and quintuplers, the theoretical efficiency using QBV's is comparable or possibly larger than using Schottky-varactor diodes.

By making the width and/or the height of the barrier in the QBV-diode such that the conduction current through the device is negligible for the voltage interval defined by the pump voltage swing, the device can be modelled simply as a voltage dependent capacitance.

A QBV-diode may be fabricated in the same way as the quantum well mesa diode, but with the epitaxial GaAs/AlGaAs/GaAs material designed as indicated in Fig. 11. The AlGaAs barrier will to a large extent prevent electrons to pass through the structure and will cause a depleted region with a voltage dependent width, which is associated with a voltage dependent capacitance $C(V)$. When the diode is biased in the forward direction, the depleted region will appear on one side of the barrier, and the depletion capacitance of the device will decrease with increasing voltage. Since the diode is essentially symmetric, a reversed bias will in the same way cause a decrease of the capacitance of the device. Hence, the maximum capacitance is obtained for zero voltage and is determined by the thickness of the AlGaAs barrier. The minimum capacitance, which occurs for maximum bias voltage, is determined by the doping concentration and the extension of the low doped region "L" (see Fig. 11). In fact a similar capacitance swing vs voltage as for the Schottky-varactor diode is expected. It is obvious that in future work one should search for optimum doping profiles.

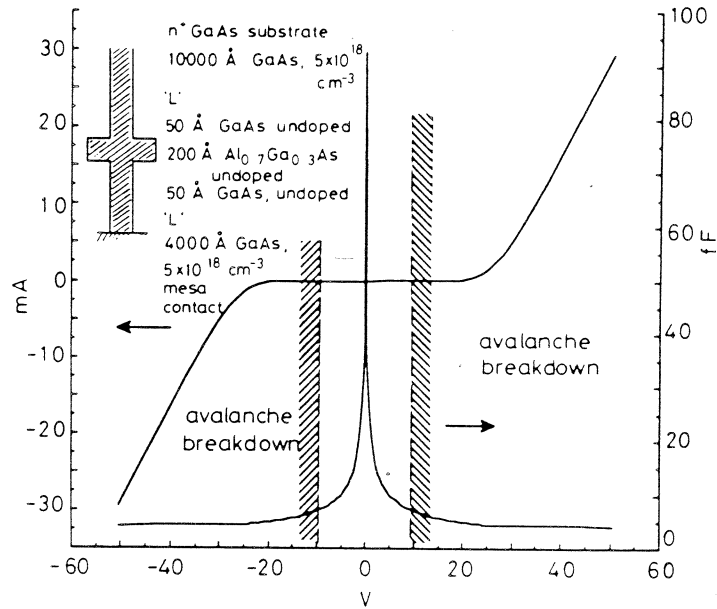


Fig.11 The doping profile of the mesa structure. Also shown is the I-V and C-V characteristic of the diode with $\varnothing=4.5$ μm , $L=4000$ \AA , and $N_D=2 \cdot 10^{17}$ cm^{-3} , assuming no avalanche breakdown. The avalanche breakdown will limit the allowable rf-voltage swing.

For the QBV-diode as well as for the Schottky-varactor diode, the series resistance $R_s(V)$ is bias dependent. In order not to overestimate the QBV-diode multiplier efficiency, we have in the calculations presented below, used a constant depletion region series resistance contribution equal to $R_{\text{depl,max}}$. Notice that for a Schottky-varactor diode tripler, the idler current at $2 \cdot \omega_p$ will deteriorate the tripler performance, since any finite reactance termination will cause power losses in the series resistance.

An I-V profile for a quantum barrier alone, consisting of $\text{Al}_{0.7}\text{Ga}_{0.3}\text{As}$ with a length of 200 \AA , has been determined from experiments [21]. Using this information, we calculated the I-V and C-V characteristics for a 4.5 μm device with this barrier followed by a 4000 \AA low doped region ($N_D=2 \cdot 10^{17}$ cm^{-3}) (see Fig. 11). Notice (Fig. 11) that the differential conductance defined as dI/dV is quite small compared to ωC .

Using a large signal multiplier analysis program based on the principle of harmonic balance developed by Siegel et. al. [18] and modified by us for the QBV-diode, the efficiency of the QBV-multiplier was calculated for a few different device structures as a function of input power. The equivalent circuit of the device and the procedure for optimization are very similar to those used for the Quantum Well multiplier in ref. [4].

The theoretical efficiency vs input power for a tripler to 105 GHz is shown in Fig. 12. The length of the region "L" is chosen to be 4000 \AA and the doping of the region is used as the parameter in Fig. 12. As mentioned above the series resistance used in these calculations is $R_s = R_{\text{depl,max}} + R_{\text{contact}}$, where R_{contact} is assumed equal to 3.14 Ω corresponding to a contact resistance of 0.5×10^{-6} ohm cm^2 . The results presented in Fig. 12 show that the conversion efficiency is high for low input

powers using low doping in the depletion region. The highest efficiency of 54 % was obtained for $N_D=2 \cdot 10^{17}$ yielding a series resistance of 19.2 Ω (see Fig. 2). This result is comparable to the maximum efficiency of 60 % theoretically and 28 % experimentally for a 3x35 GHz Schottky-varactor tripler [22] with a series resistance of 10 Ω . We found that the maximum efficiency for a QBV-diode having a series resistance of 10 Ω is 64 %. It can be seen that the series resistance does play an important part in achieving optimum efficiency for a QBV-multiplier, which of course is also the case for a Schottky-varactor multiplier. A preliminary investigation of the QBV quintupler (output frequency 175 GHz), indicates efficiencies of more than 30 %. For a 175 GHz optimum Schottky-varactor quintupler a theoretical efficiency of 30 - 40 % has been predicted for the case when all idlers have optimum reactance loads, and 15 - 25 % when two idlers are optimized [22].

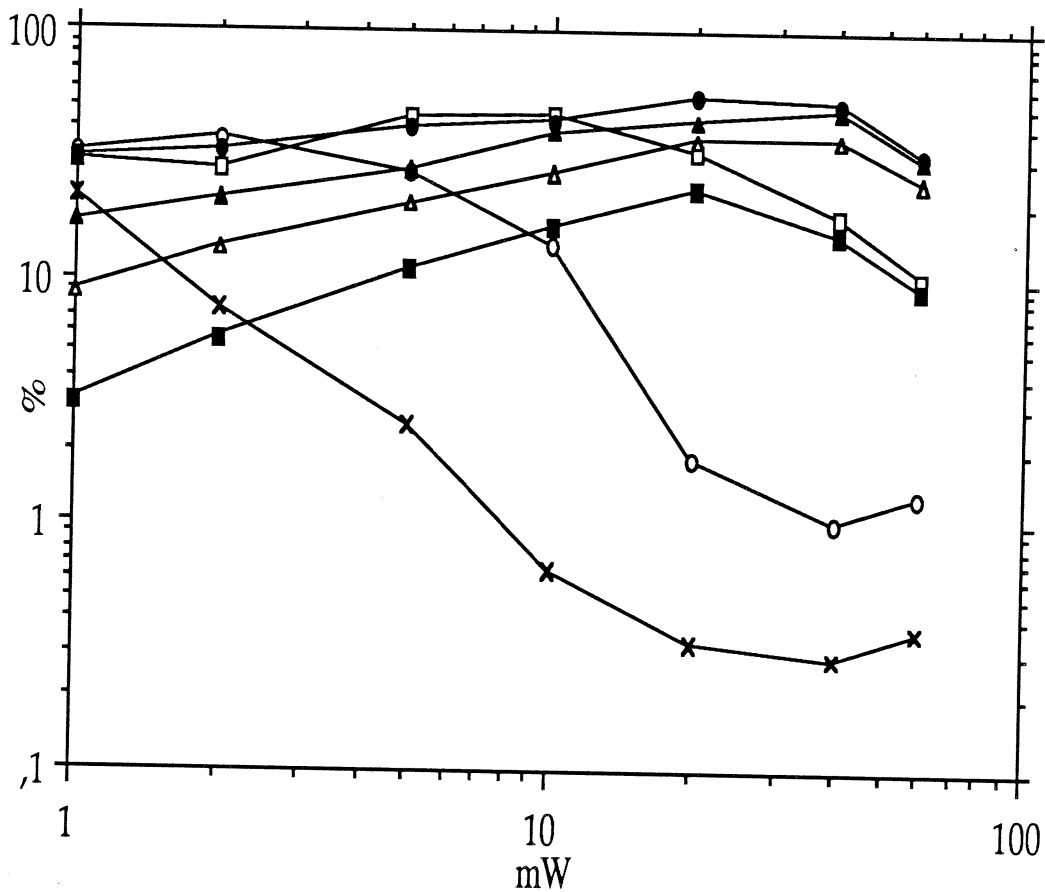


Fig. 12. Efficiency vs input power for a QBV-tripler. The doping N_D of region "L" in Fig. 1 is used as the parameter. The length of "L" is 4000 \AA .

- (X): $N_d = 1 \cdot 10^{16} \text{cm}^{-3}$, $R_s = 51.2 \Omega$.
- (O): $N_d = 2 \cdot 10^{16} \text{cm}^{-3}$, $R_s = 37.1 \Omega$.
- (□): $N_d = 4 \cdot 10^{16} \text{cm}^{-3}$, $R_s = 25.5 \Omega$.
- (●): $N_d = 8 \cdot 10^{16} \text{cm}^{-3}$, $R_s = 19.2 \Omega$.
- (▲): $N_d = 2 \cdot 10^{17} \text{cm}^{-3}$, $R_s = 15.1 \Omega$.
- (△): $N_d = 4 \cdot 10^{17} \text{cm}^{-3}$, $R_s = 13.5 \Omega$.
- (■): $N_d = 8 \cdot 10^{17} \text{cm}^{-3}$, $R_s = 12.6 \Omega$.

It is essential also that the ohmic contact is reasonably good, although at the high frequencies involved even a contact with poor dc-qualities will work well [23]. The optimum doping profile may actually be different for different frequencies of operation. The reason is that the doping profile has an influence on not only $C(V)$, but also on the I-V characteristic, i. e. the conductance $G(V)=dI/dV$, which is in parallel with $C(V)$. As a rule of thumb, G ought to be small as compared to the minimum parallel susceptance ωC for the whole bias voltage range.

We here fabricated a first batch of $\varnothing = 3 \mu\text{m}$ QBV-diodes using MBE-material (from IMEC in Leuven, Belgium). The barrier consist of 210 \AA AlGaAs with 70% Al. Outside the barrier a 50 \AA undoped spacer layer of GaAs is grown. Outside these spacer layers on each side 5300 \AA region of GaAs is grown, doped to $1 \cdot 10^{17} \text{ cm}^{-3}$ followed by highly doped GaAs to provide good ohmic contacts. The initially measured IV-characteristics showed a current density about $8 \cdot 10^5$ times larger than expected. We intend to address this problem in the near future.

Despite the too large current density, the conversion efficiency was reasonably high. The experiments were conducted in a Schottky-varactor waveguide tripler structure of the same design as described in Ref.[17]. For an output frequency of 225 GHz a maximum efficiency of more than 5 % and an output power of more than 2 mW was measured. For a good Schottky-varactor diode tripler for the same frequency, using diodes from Univ. of Virginia (type 6P2), an efficiency of about 4.5 % was obtained. A theoretical analysis of the efficiency of the used diodes yielded $\eta \approx 6.4 \%$, while a diode with the expected smaller current should offer $\eta \approx 13.6 \%$ efficiency for 32 mW input power. An ohmic contact resistance for the mesas of $3 \cdot 10^{-6} \text{ ohm cm}^2$ was assumed in the analyze [4].

12. Conclusions.

The work on applications of QW-diodes for millimeter waves and submillimeter waves have only started. Although the oscillator power obtained experimentally so far is low, it is sufficient in some applications such as for local oscillators in superconducting mixers or as a signal source for measurement systems. The main design problems are related to the device itself and the mm/submm-wave circuit, which should yield the optimum embedding impedance(s) required by the device. Besides oscillators and multipliers, mixers with gain can be constructed. However, it is not yet known whether it will be possible to achieve low mixer noise.

The QBV-diode is potentially a very competitive device in millimeter-wave multiplier applications. The obtainable multiplier efficiency with a QBV-diode is shown to be comparable to corresponding Schottky-varactor multipliers. The main advantage is that idler tuning is not required for a tripler, and only one (two) idler(-s) has to be considered for a quintupler (heptupler).

13. Acknowledgements.

The author would like to thank Dr. T. Andersson and Mr. J. Söderström for their kind supply of MBE-material for the experimental quantum well diodes and Prof. S. Yngvesson for useful discussions. Milena Mattas is acknowledged for her help in drawing most of the figures. The Swedish board for Technical Development and the European Space Agency (ESTEC contract RFQ/3-6172/88/NL/PB) are acknowledged for financial support.

References.

- [1] T. C. L. G. Sollner, E. R. Brown, W. D. Goodhue and H. Q. Le, "Observations of millimeter-wave oscillations from resonant tunneling diodes and some theoretical considerations of ultimate frequency limits," *Appl. Phys. Lett.*, vol. 50, pp. 332 - 334, 1987.
- [2] A. Rydberg, H. Grönqvist, E. Kollberg, "A theoretical and experimental investigation on millimeter-wave quantum well oscillators," *Microwave and Optical Technology letters*, vol. 1, pp. 333 - 336, 1988.
- [3] L. L. Chang, L. Esaki, R. Tsu, "Resonant Tunneling in Semiconductor Double Barriers," *Appl. Phys. Lett.*, vol. 24, pp. 593 - 595, 1974.
- [4] A. Rydberg and H. Grönqvist, "Quantum well high efficiency millimeter-wave frequency tripler," *El. Lett.* vol. 25, pp. 348 - 349, 1989.
- [5] A. Mortatzawi, V. P. Kesan, D. P. Neikirk, and T. Itoh, "A self oscillating QWITT diode mixer", to be published in the Proceedings of the 19th European Microwave Conference, London, 1989.
- [6] E. Kollberg, "Superconducting Devices and Quantum Well Diodes in Low Noise Heterodyne Receivers, Part 2: Quantum Well Diodes", *Alta Frequenza*, Vol. LVIII, No. 5-6, pp. 521-530, 1989.
- [7] V. P. Kesan, D. P. Neikirk, P. A. Blakey, B. G. Streetman and T. D. Linton, "The influence of transit-time effects on the optimum design and maximum oscillation frequency of quantum well oscillators," *IEEE Trans. on Electron Devices*, vol. ED-35, pp. 405 - 413, 1988.
- [8] E. R. Carlson, M. V. Schneider and T. F. McMaster, "Subharmonically pumped millimeter-wave mixers," *IEEE Trans. Microwave Theory and Techniques*, vol. MTT-26, pp. 706 - 715, 1978.
- [9] E. R. Brown, W. D. Goodhue and T. C. L. G. Sollner, "Fundamental oscillations up to 200 GHz in resonant tunneling diodes and new estimates of their maximum oscillation frequency from stationary-state tunnel theory," *J. Appl. Phys.*, vol. 64, pp. 1519 - 1529, 1988.
- [10] H. Grönqvist, A. Rydberg, H. Hjelmgren, H. Zirath, E. Kollberg, J. Söderström, and T. Andersson, "A millimeter wave quantum well diode oscillator," *Proceedings 18th European Microwave Conference*, Stockholm, pp. 370-375, 1988.
- [11] M. A. Lee, B. Easter, and H. A. Bell, *Tunnel diodes*, Chapman and Hall, London, 1967.
- [12] J.Y-F. Tang and K. Hess, "Investigation of Transient Electronic Transport in GaAs Following High Energy Injection.", *IEEE Trans. Electron Devices*, Vol. ED-29, pp. 1906-1911, 1982.

- [13] "Landolt-Börnstein, Numerical Data and Functional Relationships in Science and Technology.", Vol.17a, Springer-Verlag Berlin, 1982.
- [14] T.G. Andersson, Z.G. Chen, V.D. Kulakovskii, A. Uddin, J.T. Vallin, "Variation of the Critical Layer Thickness with In Content in Strained In_xGa_{1-x}As-GaAs Quantum Wells Grown by Molecular Beam Epitaxy.", Appl. Phys. Lett. Vol.51, pp.752-754, 1987.
- [15] S.M. Sze, "Physics of Semiconductor Devices.", Wiley, 1981.
- [16] J.R. Söderström, D.H. Chow, T.C. McGill, "InAs/AlSb Double Barrier Structure with Large Peak-to-Valley Ratio: A Candidate for High Frequency Microwave Devices.", To be published.
- [17] N.R. Erickson, "A high frequency tripler for 230 GHz," Proc. European Microwave Conf. 1982, pp. 288-292.
- [18] P.H. Siegel, A.R. Kerr and W. Hwang, "Topics in the Optimization of Millimeter Wave Mixers," Nasa Technical Paper 2287, March 1984.
- [19] A. Rydberg, "On the Design of Quantum-Well Multipliers", Proc. 14th International Conference on Infrared and Millimeter Waves, Würzburg, BRD, pp. 467-468, 1989.
- [20] E. Kollberg and A. Rydberg, "Quantum-Barrier-Varactor Diodes for High Efficiency Millimeter-Wave Multipliers.", Electronics Letters, Vol. 25, No. 25, pp. 1696-1697, 1989.
- [21] I. Hase, H. Kawai, K. Kaneko and N. Watanabe, "Electron transport through the MOCVD grown GaAs/AlGaAs/GaAs heterojunction barrier," Electronics Lett., vol. 20, pp. 491-492, 1984.
- [22] T.J. Tolmunen, "High efficiency Schottky-varactor frequency multipliers at millimeter waves," Thesis for doctor of Technology degree, Helsinki University of Technology, Report S 180, 1989. (Partly published in Int. J. of Infrared and Millimeter Waves, vol. 8, pp. 1313 - 1353 (1987) and vol 9, pp. 475 - 518 (1989))
- [23] H. Zirath, "On the high-frequency behaviour of ohmic contacts," Proc. 19'th European Solid State Device Research Conference ESSDERC'89, Berlin, BRD, pp. 63-66, 1989.